

Saccharin Dependence of Magnetoimpedance Ratio in Electrodeposited Permalloy Multilayer Structure on Meandered-Copper Printed-Circuit-Board Substrates

Artono Dwijo Sutomo^{1,*}, Pratiwi Kusumawardhani¹,
Hana Hanifah Yasmin¹, Restu Handayani¹, Yusri¹, Ismail², Utari¹,
Ari Handono Ramelan¹, Nuryani¹ and Budi Purnama¹

¹Department of Physics, Faculty of Mathematics and Natural Sciences, Universitas Sebelas Maret, Surakarta 57126, Indonesia

²Polytechnics Institute of Nuclear Technology, Yogyakarta 55281, Indonesia

(*Corresponding author's e-mail: artono@staff.uns.ac.id)

Received: 4 February 2023, Revised: 11 March 2023, Accepted: 17 April 2023, Published: 28 August 2023

Abstract

The effect of saccharin concentration on magnetoimpedance ratio in multilayer permalloy structure i.e., [NiFe/Cu/NiFe]₃/Cu/[NiFe/Cu/NiFe]₃ on Cu printed circuit board (PCB) meander substrates have been discussed. The multilayer [NiFe/Cu/NiFe]₃/Cu/[NiFe/Cu/NiFe]₃ structure was prepared by using the electrodeposition method. The results of XRF characterization show that the composition of Ni:Fe is close to the calculation mol ratio permalloy of 80:20. The magnetoimpedance effect is evaluated by total impedance measurement at the various magnetic fields. The typical increase of the magneto-impedance ratio with frequency confirms in this experiment. Here, the magnetoimpedance ratio modifies from 0.07 to 1.63 % for frequency measurements of 20 and 100 kHz, respectively. Finally, the MI ratio monotonically decreases with an increase in additive saccharin concentration. The MI ratio slightly decreases by 17.17 % $(=(1.63-1.35)/1.63)$ for additive saccharin concentration increase of 1 to 2 g/L. Then MI ratio drastically decreases by 40.0 % $(=(1.35-0.81)/1.35)$ in the change of additive saccharin concentration from 2 to 4 g/L. Here, the change in the morphological surface should attribute to the decrease in the MI ratio.

Keywords: Electro-deposition, Magneto-impedance, Multilayer, NiFe, Cu PCB, Meander, Saccharin

Introduction

The Magneto Impedance (MI) effect is the change in the electrical impedance of a soft magnetic material when it is affected by an external magnetic field [1]. The effect of MI on various soft ferromagnets thin films can be obtained through such kind procedure i.e., rapid cooling deposition, electrodeposition, magnetron sputtering, and other methods [2]. The MI effect has been studied extensively for magnetic sensor applications such as biomedical applications due to its high sensitivity at room temperature and ease of miniaturization [3]. In biomedical applications, MI sensors can be used in conjunction with Magnetoencephalography (MEG) to detect brain activity [4]. Besides being applied in biomedical fields, MI is also applied in engineering and industrial fields, such as navigation, military and security, target detection and tracking, anti-theft systems, non-destructive testing, magnetic marking and labeling, geomagnetic measurement, research space, measurement of magnetic fields in spacecraft [5-7].

Some of the interesting characteristics i.e., high magnetic permeability, well-defined magnetic anisotropy, and low coercivity of magnetic materials required to realize a high MI phenomenon. Furthermore, the geometric structure in the multi-layer structure such kind [NiFe/Cu/NiFe], successfully improves the performance of the magnetic layer to obtain a high ratio of the MI. In the case electrodeposition procedure, the multilayer structure also may avoid the formation of a trans critical state [8,9] i.e., a maximum thickness of a single thin layer that can be well-deposited on a substrate. In addition, it has been found that the meander (winding) sample geometry has a higher MI ratio magnitude due to mutual induction between the nearest meander line [10-12]. The stress effect also is reported to modify the MI ratio [13]. Permalloy of Ni₈₀Fe₂₀ is widely used for the realization of highly sensitive MI sensors because they are soft magnetic materials with high permeability (~10000) [14]. Utilization of NiFe using a meandering pattern of Cu PCB as a substrate has been carried out in previous studies with variations in the number of N layers [15] and then, symmetry and asymmetry multilayered configuration [16].

Concerning the preparation of thin films by the electrodeposition route, organic additives have been commonly used in the electrodeposition of metals and alloys for the relaxation of residual stresses. These changes should bring a significant improvement in the magnetic properties as well as anti-corrosion thin films [17]. Saccharin is one of the organic additives known to control deposit adhesion and reduce stress on the coating [18].

This paper reports on the MI effect in multi-layer symmetry configuration of $[\text{NiFe}/\text{Cu}/\text{NiFe}]_3/\text{Cu}/[\text{NiFe}/\text{Cu}/\text{NiFe}]_3$ electrodeposited Cu PCB meander pattern. The additive material of saccharin as a deposition variable is used to modify the physical properties as well as the MI phenomenon. The MI is performed by measurement of the total impedance at various magnetic fields on the multilayer sample for low frequency (≤ 100 kHz).

Materials and methods

In this study, a technical Cu PCB substrate with a meander pattern is used throughout the whole experiment. The meander pattern on the Cu PCB substrate is shown in **Figure 1**. The meander line width is $250 \mu\text{m}$, the distance between the meander lines is also $250 \mu\text{m}$, and the overall line length is 28.7 cm. The substrate is cleaned with an ultrasonic cleaner for 30 min before the electrodeposition process. Two types of solutions are used in the electrodeposition process, namely NiFe solution and Cu solution. NiFe electrolyte solution was made from a mixture of $\text{NiSO}_4 \cdot 6\text{H}_2\text{O}$ (Merck), FeSO_4 (Merck), H_3BO_3 (Merck), $\text{C}_7\text{H}_5\text{NO}_3\text{S}$ (Merck), and $\text{C}_{12}\text{H}_{25}\text{NaO}_4\text{S}$ (Merck). Meanwhile, the Cu electrolyte solution was made from a mixture of CuSO_4 (Merck), $\text{C}_7\text{H}_5\text{NO}_3\text{S}$ (Merck), and $\text{C}_{12}\text{H}_{25}\text{NaO}_4\text{S}$ (Merck). The stoichiometric of the solution used for NiFe layer and Cu layer are depicted at **Table 1**. All ingredients were dissolved in 100 mL of distilled water. In order to modify the physical properties of the multilayer sample, variations in the amount of saccharin mass ($\text{C}_7\text{H}_5\text{NO}_3\text{S}$) add to the electrolyte solution.

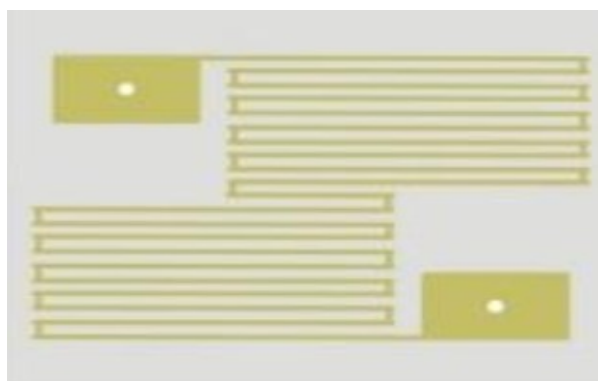


Figure 1 The meander pattern on the Cu PCB substrate.

Table 1 The stoichiometric calculation for deposition of NiFe and Cu layers

Solution	Concentration
$\text{NiSO}_4 \cdot 6\text{H}_2\text{O}$	0.099 M
$\text{FeSO}_4 \cdot 7\text{H}_2\text{O}$	0.012 M
$\text{CuSO}_4 \cdot 5\text{H}_2\text{O}$	0.065 M
H_3BO_3	0.149 M
$\text{C}_{12}\text{H}_{25}\text{NaO}_4\text{S}$	1 g/L
$\text{C}_7\text{H}_5\text{NO}_3\text{S}$	1 - 4 g/L

The electrodeposition process is carried out by passing a current through the platinum and Cu PCBs, which act as anodes and cathodes, respectively. The deposition process in NiFe solution was carried out with a current density of $15.5 \text{ mA}/\text{cm}^2$. Meanwhile, the deposition of Cu solution was carried out with a current density of $8 \text{ mA}/\text{cm}^2$. The multilayer deposition procedure was started by electrodeposited NiFe films, followed by a Cu layer, and then electrodeposited NiFe film again. Here, the multilayer of $[\text{NiFe}/\text{Cu}/\text{NiFe}]$ with a repetition number of $N = 1$ is obtained. Thereafter, the procedure is repeated until the desired multilayer system of $[\text{NiFe}/\text{Cu}/\text{NiFe}]_3/\text{Cu}/[\text{NiFe}/\text{Cu}/\text{NiFe}]_3$ is obtained.

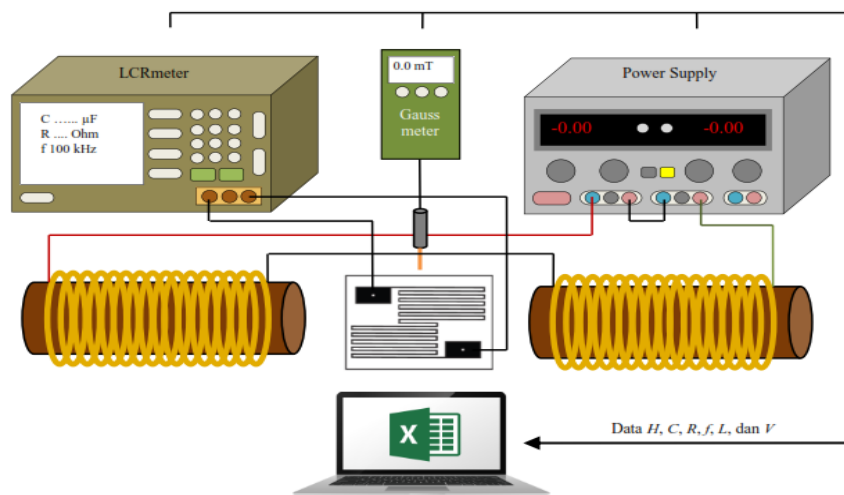


Figure 2 Experimental schematic of the measurement of MI effects.

The obtained film samples were evaluated for crystalline structure by using the element composition by using X-Ray Fluorescence (XRF) and X-Ray Diffractometer (XRD). Then, MI measurements are carried out by measurement of a total impedance, $Z = \sqrt{R^2 + X^2}$ under several magnetic field. Here, the Z of the multilayer sample calculate following the values of resistance (R), capacitance (C), and inductance (L) for a given frequency (f) i.e., 20 - 100 kHz. The MI ratio to total impedance when given an external magnetic field (H), is calculated using equation $\Delta Z/Z(\%) = (Z(H) - Z(H_{max})/Z(H_{max}) \times 100 \%$. **Figure 2** shows the experimental schematic of the measurement of MI effects.

Results and discussion

Determination of the deposition rate in this study using the gravimetric method. The principle of this method is to weigh the mass of NiFe and Cu coated on the substrate to determine the thickness of the thin layer. The gravimetric method is used to determine the difference in mass of the substrate before and after being coated to be used in calculating the coating thickness. The equation used to determine the layer thickness using the gravimetric method is shown in Eq. (1).

$$t = \frac{\Delta m}{A\rho} \tag{1}$$

where Δm is the difference in mass before and after the electrodeposition process, and A is the area of the substrate and its density. The density used for NiFe is 8.75 g/cm³ and the density of Cu is 8.94 g/cm³ [16].

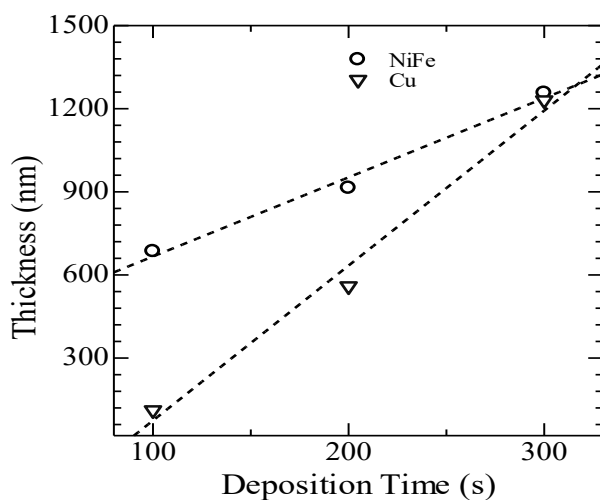


Figure 3 The thickness of the NiFe and Cu layers as a function of time electrodeposition.

Figure 3 shows the dependence of the time of deposition on the thickness of the NiFe and Cu layers formed on the substrate. The NiFe layer is formed from the electrodeposition process using the current density $J = 15.5 \text{ mA/cm}^2$ and a voltage of 3.5 Volts. While the Cu layer is in electrodeposition using current density $J = 8 \text{ mA/cm}^2$ and potential difference $V = 3 \text{ Volt}$. Both electrodeposition processes were carried out with the addition of 4 g/L saccharin in NiFe and Cu electrolyte solutions. Based on **Figure 3**, the layer thickness increases linearly with increasing time. These results indicate that the thickness thin layer can be controlled by deposition time. It can also be seen that the NiFe curve is gentler than the Cu curve. This shows that the rate of NiFe is slower than Cu.

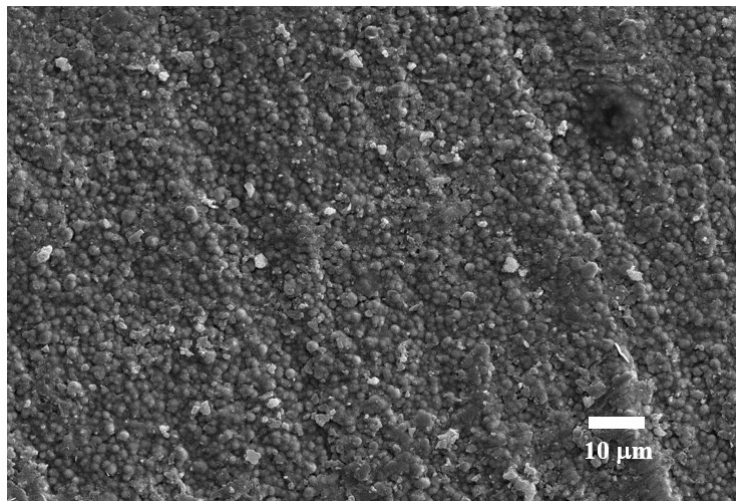


Figure 4 Typical surface morphology of the NiFe layer electrodeposited on Cu PCB substrate.

The linear graph in **Figure 3** is viewed as the equation $y = mx + C$, then the gradient of the equation shows the deposition rate at the time electrodeposition takes place. The deposition rate obtained for the NiFe layer is 2.86 nm/s while the deposition rate for the Cu layer is 5.59 nm/s with the gradient equation $y = mx + C$ the NiFe layer is $y = 2.86x + 3.80$ and $y = 5.59x + 4.85$ for the Cu layer. The value of the constant (C) in the graph equation indicates the distance the gradient line shifts to the point (0,0).

XRF test was carried out to determine the elemental composition deposited from the growth of a thin layer of electrodeposition. Characterized samples a sample of NiFe coating produced from electrodeposition with the addition of saccharin as much as 4 g/L. The deposited sample has a layer thickness of 300, 500, 700 and 900 nm. The thickness of thin films was determined by controlled deposition time and rate, it is known using the equation $y = mx + c$ where m is the deposition rate, y is the layer thickness, and x is the deposition time.

A thin layer with a thickness of 300 nm has a Ni:Fe composition percentage of 80:20. In a thin layer with a thickness of 500 nm has a Ni:Fe composition percentage of 65.68:20. The percentage composition of Ni:Fe in a layer with a thickness of 700 nm is of 77.4:20 and a thin layer with a thickness of 900 nm has a Ni: Fe composition percentage of 79.27:20. Based on the 4 variations in the thickness of the thin layer above, the overall percentage of Ni:Fe composition obtained is almost 80:20, which is the percentage of the permalloy composition. The most similar percentage of permalloy composition is found at 300 nm thickness. This is in accordance with the research conducted by Salman [19] which obtained the percentage composition of Ni:Fe of 79.34:20.66 and 80.32:19.68 where both results are also close to the percentage of Ni:Fe permalloy composition = 80:20 [16].

Figure 4 shows the typical surface morphology of the NiFe layer electrodeposited on a technical Cu printed circuit board (PCB) substrate. The relatively homogeneous surface morphology of the sample confirms that the thin film/layer formation process takes place simultaneously. This is supported by the presence of relatively the same grains. Meanwhile, the presence of some kind of elongated defects is unavoidable because of the use of technical PCB Cu substrates.

Characterization using X-Ray Diffraction (XRD) was carried out to confirm that the thin layer deposited was Ni-Fe permalloy. Results characterization with XRD is displayed in the form of a diffraction pattern with a graph of the relationship between the diffraction angles (2θ) taken from 30 - 60 ° with intensity (I) as shown in **Figure 5**.

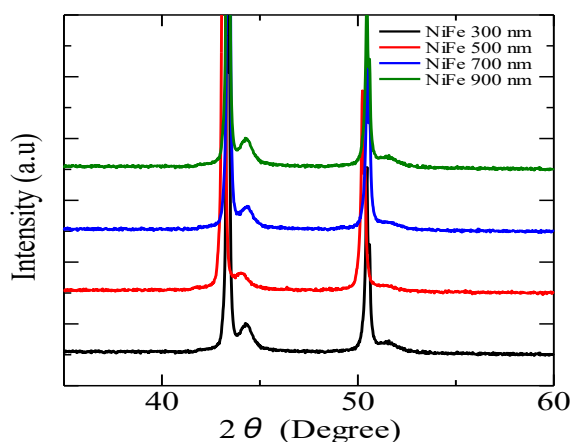


Figure 5 XRD test results on NiFe layers with a thickness of 300, 500, 700 and 900 nm.

Figure 5 shows the X-ray diffraction pattern of a NiFe sample with 300, 500, 700 and 900 nm layer thickness variations in the display SMA4win program. From the XRD results, it can be seen that the diffraction pattern is the same although each NiFe thin layer has a different thickness. The characteristic peak angle of the NiFe layer in the 4 variations of sample thickness is shown in **Table 2**.

Table 2 The characteristic peaks of the 300, 500, 700 nm and thickness samples 900 nm.

Sample Thickness (nm)	2θ (°)
300	44.25
500	44.04
700	44.36
900	44.25

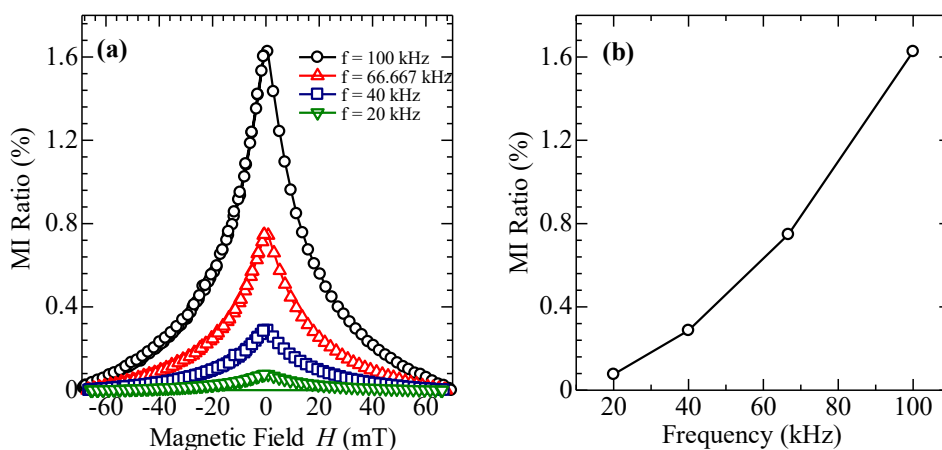


Figure 6 (a) Multilayer MI curve $[NiFe/Cu/NiFe]_3/Cu/[NiFe/Cu/NiFe]_3$ with variations in frequency (b) Graph of the effect of frequency on the MI ratio.

The diffraction spectral for the typical variation of the thickness layer is obtained at the angle of about $2\theta \approx 44.2^\circ$ with Miller index hkl (111). The results are in agreement with the International Center for Diffraction Data (ICDD) database number 471417. The presence of another peak in **Figure 6** is due to the Cu PCB used as a substrate. The characteristic peak of the angle 2θ obtained is also according to research conducted by Han *et al.* which shows that the NiFe permalloy has a peak characteristic at an angle of $2\theta \approx 44.3^\circ$ with Miller index hkl (111) [20]. This peak result is also under research by Subramanian *et al.* which

has a diffraction peak at the index Miller hkl (111) [21]. This indicates that the layer formed on the PCB Cu substrate from this electrodeposition result is NiFe permalloy.

In this study, the frequency variation of $[\text{NiFe/Cu/NiFe}]_3/\text{Cu}/[\text{NiFe/Cu/NiFe}]_3$ with symmetrical electrodeposition was carried out on a meander pattern of Cu PCB substrate with the addition of saccharin 1 g/L additive to determine its effect on the MI ratio. NiFe has a thickness of 600 nm and Cu has a thickness of 150 nm. MI measurements are carried out using low frequencies with a frequency range from 20 - 100 kHz. The change in voltage across the sample during low-frequency measurements is due to the magneto-inductive effect. The skin effect under these conditions is very weak so the change in sample impedance on the application of a magnetic field results from the contribution of inductance (L) which is proportional to the planar magnetic permeability of the layer [7].

A typical magnetoimpedance curve with a symmetric structure $N = 3$ is obtained from data processing by the SMA4win program. **Figure 6(a)**, shows the results measurement of the MI ratio as a function of the external magnetic field. It is seen that when no external magnetic field is applied, the magnetoimpedance ratio reaches its peak at each frequency. However, when a magnetic field is applied ($H > 0$) the magnetoimpedance ratio decreases until the value of the magnetic field is constant at around 60 mT.

Figure 6(b), shows the MI ratio increases with increasing frequency. At the lowest frequency (20 kHz) the MI ratio is 0.07 %. Furthermore, the MI ratio changed to 0.29 % at a frequency of 40 kHz and 0.75 % at a frequency of 66.67 kHz. The MI ratio reaches its maximum peak at 100 kHz frequency, which is 1.63 %. The large MI value can be caused by the use of magnetic materials that have large permeability, small skin depth, and small DC resistance. As the frequency increases, the permeability will increase and there will be a decrease in skin depth which is then increased by the applied field so that a higher MI ratio is obtained [7].

Figure 7(a) shows the results of the MI ratio measurement with variations in saccharin mass at a frequency of 100 kHz as a function of the external magnetic field to the MI ratio. The mass variation of saccharin used in this study was 1 - 4 g/L.

It can be seen in **Figure 7(b)** that when the mass of saccharin increases, the MI ratio will decrease. From the measurement results in the figure, it was observed that the highest MI ratio was obtained when the saccharin mass used was 1 g/L with a ratio value of 1.63 %. Furthermore, the MI ratio was reduced by a value of 1.61 % with the use of saccharin 2 g/L and 1.35 % in the mass of saccharin 3 g/L. The lowest MI ratio value of 0.81 % was obtained at 4 g/L saccharin mass. From the measurement results, it was observed that the MI ratio when the saccharin 1 and 2 g/L coincided, indicating that the difference in the MI ratio values between the 2 was not very significant. This can happen because that position has experienced saturation. The results of this study are in accordance with the research conducted by Mishra [17], who found that the ratio $(\Delta Z/Z)\%$ max was optimum when the saccharin mass was 1 g/L [17].

Electrodeposition with the addition of saccharin to the solution can help level the surface, reduce the internal stress of the deposit, and reduce grain size. However, the excessive addition of saccharin in the electrolyte solution causes a non-uniform microstructure and a bimodal size distribution resulting in surface roughening [22]. The decrease in the MI ratio with the addition of saccharin was due to changes in magnetic properties due to changes in the microstructure of the layer formed [17]. As a result, there is a change in the magnetic domain structure and the spin relaxation attenuation decreases with decreasing anisotropy.

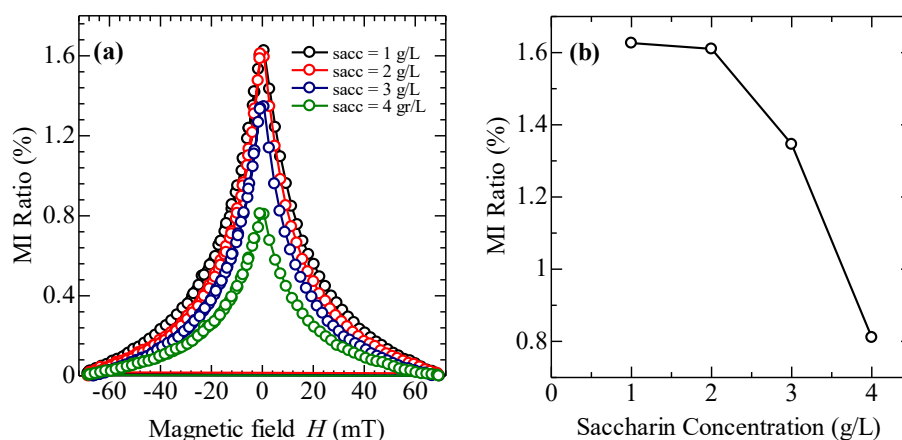


Figure 7 (a) Multilayer MI curve of $[\text{NiFe/Cu/NiFe}]_3/\text{Cu}/[\text{NiFe/Cu/NiFe}]_3$ with variations in saccharin mass (b) Graph of the effect of saccharin mass on MI ratio.

Conclusions

The effect of saccharin solution to magnetoimpedance ratio in multilayer $[\text{NiFe}/\text{Cu}/\text{NiFe}]_3/\text{Cu}/[\text{NiFe}/\text{Cu}/\text{NiFe}]_3$ structure on Cu PCB meander substrates has been evaluated. The magnetoimpedance effect is evaluated by total impedance measurement at the various magnetic fields. The typical increase of the magneto-impedance ratio (MI) with frequency confirm in this experiment. Here, the MI ratio modifies from 0.07 to 1.63 % for frequency measurements of 20 and 100 kHz, respectively. Finally, the MI ratio monotonically decreases with an increase in additive saccharin concentration. The MI ratio slightly decreases by 17.17 % $(=(1.63-1.35)/1.63)$ for additive saccharin concentration increase of 1 to 2 g/L. Then MI ratio drastically decreases by 40.0 % $(=(1.35-0.81)/1.35)$ in the change of additive saccharin concentration from 2 to 4 g/L. Here, the change in the morphological surface should attribute to the decrease in the MI ratio.

References

- [1] A Sayad, SM Uddin, J Chan, E Skafidas and P Kwan. Meander thin-film biosensor fabrication to investigate the influence of structural parameters on the magneto-impedance effect. *Sensors* 2021; **21**, 6514.
- [2] A García-Arribas, E Fernández, A Svalov, GV Kurlyandskaya and JM Barandiaran. Thin-film magneto-impedance structures with very large sensitivity. *J. Magn. Magn. Mater.* 2016; **400**, 321-6.4
- [3] A Sayad, E Skafidas and P Kwan. Magneto-impedance biosensor sensitivity: Effect and Enhancement. *Sensors* 2020; **20**, 5213.
- [4] K Wang, S Tajima, Y Asano, Y Okuda, N Hamada, C Cai and T Uchiyama. Detection of P300 brain waves using a magneto-impedance sensor. *Int. J. Smart Sens. Intell. Syst.* 2014; **7**, 1-4.
- [5] Y Wang, Y Wen, F Song, P Li and S Yu. Enhanced inductance in laminated multilayer magnetic planar inductor for sensitive magnetic field detection. *Appl. Phys. Lett.* 2018; **112**, 182403.
- [6] O Thiabgoh, T Eggers, SD Jiang, JF Sun and MH Phan. Condition monitoring and failure prediction of gear rotation using a contactless RF magnetic sensor. *J. Electron. Mater.* 2019; **48**, 4000.
- [7] MH Phan and HX Peng. Giant magnetoimpedance materials: Fundamentals and applications. *Progr. Mater. Sci.* 2008; **53**, 323-420.
- [8] B Li, MN Kavaldzhiev and J Kosel. Flexible magnetoimpedance sensor. *J. Magn. Magn. Mater.* 2015; **378**, 499-505.
- [9] LV Panina and K Mohri. Magneto-impedance in multilayer films. *Sensor. Actuator. Phys.* 2000; **81**, 71.
- [10] Z Zhou, Y Zhou and Y Cao. The investigation of giant magnetoimpedance effect in meander NiFe/Cu/NiFe film. *J. Magn. Magn. Mater.* 2008; **320**, e967.
- [11] T Wang, L Guo, C Lei and Y Zhou. Detection of the magnetite by giant magnetoimpedance sensor. *Mater. Lett.* 2015; **158**, 155-8.
- [12] H Kikuchi, M Tani and T Umezaki. Effects of parallel and meander configuration on thin-film magnetoimpedance element. *AIP Adv.* 2020; **10**, 015334.
- [13] ASD Melo, F Bohn, A Ferreira, F Vaz and MA Correa. High-frequency magnetoimpedance effect in meander-line trilayered films. *J. Magn. Magn. Mater.* 2020; **515**, 167166.
- [14] T Wang, Y Zhou, C Lei, J Lei and Yang, Z. Development of an ingenious method for determination of Dynabeads protein A based on a giant magnetoimpedance sensor. *Sensor. Actuator. B Chem.* 2013; **186**, 727.
- [15] V Oktaria and B Purnama. Influence of multilayer number to magnetoimpedance ratio in electrodeposited $[\text{NiFe}/\text{Cu}]_N$ Multilayer. *Key Eng. Mater.* 2020; **855**, 191-6.
- [16] DA Rusydhan, CT Putra, AD Sutomo and B Purnama. Magnetoimpedance effect in symmetry and non-symmetry multi lapisans $[\text{Ni}_{80}\text{Fe}_{20}/\text{Cu}]_x/\text{Cu}/[\text{Ni}_{80}\text{Fe}_{20}/\text{Cu}]_{6-x}$ on PCB Cu substrate. *J. Phys. Conf. Ser.* 2021; **1951**, 012025.
- [17] AC Mishra, T Sahoo, V Srinivas and AK Thakur. Microstructure, magnetic, and magnetoimpedance properties of electrodeposited NiFe/Cu and CoNiFe/Cu wire: A study on influence of saccharin additive in plating bath. *J. Appl. Phys.* 2011; **109**, 073901.
- [18] S Esmaili, ME Bahrololoom and Zamani, C. Electrodeposition of NiFe/Cu multi lapisans from a single bath. *Surf. Eng. Appl. Electrochem.* 2011; **47**, 107-111.
- [19] A Salman, R Sharif, K Javed, S Shahzadi, KT Kubra, A Butt, S Saeed, H Arshad, S Parajuli, J Feng. Controlled electrochemical synthesis and magnetic characterization of permalloy nanotubes. *J. Alloy. Comp.* 2020; **836**, 155434.

-
- [20] Y Han, X Li, WX Lv, WH Xie, Q Zhao and ZJ Zhao. Magnetoimpedance effect of FINEMET ribbons coated with Fe₂₀Ni₈₀ permalloy film. *J. Alloy. Comp.* 2016; **678**, 494-8.
- [21] B Subramanian, K Govindan, V Swaminathan and M Jayachandran. Materials properties of electrodeposited NiFe and NiCoFe coatings. *Trans. IMF* 2009; **87**, 325-9.
- [22] SH Kim, HJ Sohn, YC Joo, WE Kim, TH Yim, HY Lee and T Kang. Effect of saccharin addition on the microstructure of electrodeposited Fe-36 wt.% Ni alloy. *Surf. Coat. Tech.* 2005; **199**, 43-8.